THE JOURNAL OF PHYSICAL CHEMISTRY C
A JOURNAL OF THE AMERICAN CHEMICAL SOCIETY

pubs.acs.org/JPCC

Article

Manifestation of Stoichiometry Deviation in Silica-Coated Magnetite Nanoparticles

Sergey V. Stolyar, Roman N. Yaroslavtsev,* Anna V. Tyumentseva, Sergey V. Komogortsev, Ekaterina S. Tyutrina, Alina T. Saitova, Yulia V. Gerasimova, Dmitriy A. Velikanov, Michael V. Rautskii, and Rauf S. Iskhakov

Cite This: *J. Phys. Chem. C* 2022, 126, 7510−7516

Read Online

ABSTRACT: Iron oxide nanoparticles were synthesized by the coprecipitation method. Two varying Fe_3O_4/tetraethoxysilane ratios were used for silanization: 1:1.3 and 1:4.5. The samples were investigated using transmission electron microscopy, ferromagnetic resonance, IR spectroscopy, and magnetometry. Magnetic measurements have shown that the magnetite core in nanoparticles has a higher magnetization than stoichiometric magnetite nanoparticles of the same size. The increased magnetization was caused by the deviation of the magnetite stoichiometry due to the interaction with the silicate coating. The blocking temperature distribution was determined from the temperature dependence of the coercive force and from the ZFC/FC dependencies. Nanoparticles with a thicker shell have shown greater efficiency in DNA isolation.

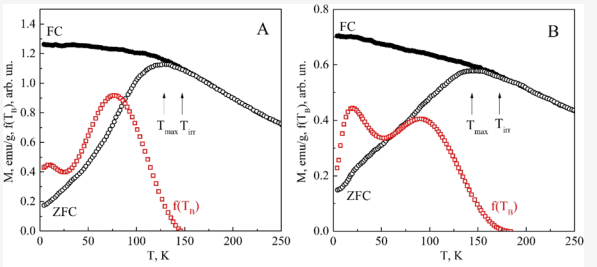

sample	X_{Fe3O4}, at synthesis (from TEM)	M_{s0}, emu/g	Estimate of M_{s0_m}, at synthesis (from TEM)
A (Fe_3O_4: SiO_2 = 1:1.3)	0.435 (0.588)	46.0 ± 0.2	105 (78.2)
B (Fe_3O_4: SiO_2 = 1:4.5)	0.182 (0.291)	10.9 ± 0.2	60 (37.5)

1. INTRODUCTION

In recent years, magnetic nanoparticles based on iron oxides have attracted interest in practical applications in the fields of biotechnology and biomedicine.[1−4] Surface-modified magnetic nanoparticles can be used for selective isolation of certain biomolecules, such as nucleic acids and proteins. The method, commonly known as "magnetic separation", has gained popularity in performing tests for diagnostic purposes.[5,6]

The development of effective methods for the separation of individual cells or molecules is an important and essential task for laboratory diagnostics today. Separation allows one to selectively analyze the components of complex biological samples, reducing non-specific signals from impurities and thereby ensuring the validity of the results of molecular genetic studies. The use of magnetic nanoparticles for the separation of biological objects (molecules, cells, etc.) has become widespread due to the ease of use, relative safety in combination with the ability to obtain a pure product, and the possibility of automating the process. Magnetic separation is one of the most specific and convenient methods. However, the development of nanoparticles requires special attention to the composition to combine the beneficial properties of the nanoparticles with their safety and biocompatibility. Thus, various studies have shown that iron oxide particles can cause oxidative stress in cells, DNA damage, and protein aggregation.[7,8] The use of various coatings makes it possible to increase the biocompatibility of nanoparticles. For the separation of biological molecules, silica coating is one of the most suitable methods because of its inertness and the ability to quickly and reversibly adsorb nucleic acids on the surface.[9] However, it is important to choose an optimal Fe_3O_4/SiO_2 ratio in the particles to ensure the densest coverage of the magnetic core and maintain magnetic properties.

Magnetic separation requires superparamagnetic particles with high saturation magnetization. The vast majority of magnetic particles used are iron oxides such as magnetite and maghemite. Iron oxide nanoparticles are characterized by sufficiently high magnetization, low reactivity, and good biocompatibility. There is a large number of works devoted to the use of iron oxide nanoparticles in magnetic separation.[10−12]

This study aimed to synthesize and investigate magnetic nanocomposites of iron oxide for the following functionalization for nucleic acid separation.

Received: January 16, 2022
Revised: April 11, 2022
Published: April 22, 2022

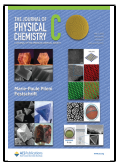

https://doi.org/10.1021/acs.jpcc.2c00349
J. Phys. Chem. C 2022, 126, 7510−7516

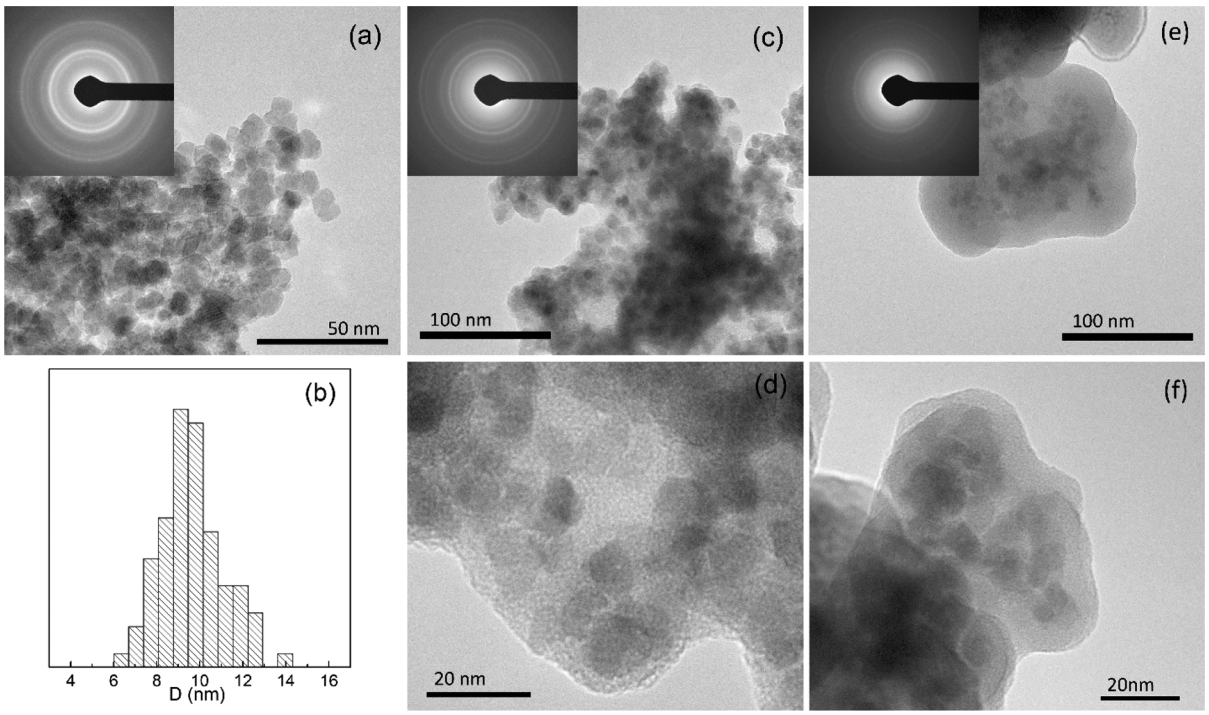

Figure 1. TEM images of magnetic nanoparticles: (a,b)—naked Fe_3O_4 nanoparticles and their size distribution and (c,d)—Fe_3O_4:SiO_2 = 1:1.3, (e,f)—Fe_3O_4/SiO_2 = 1:4.5. The insets show microdiffraction patterns.

2. EXPERIMENTAL SECTION

The synthesis of magnetic nanoparticles was carried out by the method of chemical coprecipitation of iron salts $FeCl_3$ and $FeCl_2$ in a molar ratio of 2:1 in an aqueous solution. 500 mg of the salt mixture was dissolved in 92 mL of distilled water and stirred using a mechanical stirrer for 10 min. Then, 8 mL of 25% aqueous ammonia solution was injected into the solution and incubated with constant stirring for another 30 min. The final pH after the addition of aqueous ammonia was 10−11. At the end of the synthesis, the magnetic precipitate was collected using a neodymium magnet and washed with distilled water until neutral pH was reached.

Tetraethoxysilane (TEOS) was used to coat magnetic nanoparticles with silicon oxide. Magnetic nanoparticles were coated in an ethanol/water mixture in a 9:1 ratio with the addition of TEOS in two versions: 50 mg nanoparticles per 250 μL TEOS (sample A Fe_3O_4/SiO_2 = 1:1.3) and 50 mg nanoparticles per 800 μL TEOS (sample B Fe_3O_4/SiO_2 = 1:4.5). TEOS hydrolysis and polymerization occur in the presence of water and at room temperature for several hours. After the addition of TEOS, the mixture was alkalized with 5 mL of 25% aqueous ammonia solution per 100 mL of the reaction mixture and incubated for 3 h at room temperature with continuous mechanical stirring.

Electron microscopy studies were carried out on a Hitachi HT7700 transmission electron microscope (accelerating voltage, 100 kV). Ferromagnetic resonance (FMR) spectra were measured with the X-band (9.4 GHz) spectrometer ELEXSYS E580 (Bruker, Germany). IR spectra were obtained on samples in the KBr matrix in the spectral range 350−4000 cm^{-1}. The static magnetic measurements were performed on an automated vibrating sample magnetometer in fields of up to 15 kOe at room temperature. The studies were carried out on the equipment of the Krasnoyarsk Regional Center of Research Equipment ≪Krasnoyarsk Science Center SB RAS≫.

3. RESULTS AND DISCUSSION

Figure 1 shows transmission electron microscopy (TEM)-images of Fe_3O_4 and Fe_3O_4@SiO_2 nanoparticles. The average size of the magnetite core was ∼10 nm. The diameter of the silicate coating was ∼3 nm for the Fe_3O_4/SiO_2 = 1:1.3 sample and ∼15 nm for the Fe_3O_4/SiO_2 = 1:4.5 sample. The diffraction images shown in the insets contain all reflections characteristic of magnetite. Using the shell thickness values obtained from TEM, we estimated the ratios between the magnetite core and the silicate shell: sample A Fe_3O_4/SiO_2 = 1:0.7 and sample B Fe_3O_4/SiO_2 = 1:2.4. The obtained ratios turned out to be somewhat different from the ratios at synthesis.

Figure 2 shows X-ray diffraction patterns of magnetite nanoparticles and magnetite nanoparticles coated with silica with different shell thicknesses. The diffraction patterns contain reflections characteristic of magnetite: 29.7, 35.3, 43.1, 53.4, 56.7, and 62.5°.

Figure 3 shows the FTIR spectra of magnetic nanoparticles coated with silica. Analysis of IR spectra showed the presence of Fe−O bonds (∼580 cm^{-1}). The peaks of strong stretching vibrations of siloxane groups Si−O (∼1090 cm^{-1}) and silanol groups Si−OH (∼800 and ∼950 cm^{-1}) prove the formation of a silicon oxide shell on the surface of a nanoparticle. The broad absorption band at 3400 cm^{-1} and the band at 1640 cm^{-1} correspond to the stretching and bending vibrations of adsorbed water molecules. Comparison of the spectra shows that they have the same characteristic oscillations. The main vibration band of Si−O−Si at 1090 cm^{-1} does not change its position. An increase in the intensity of the 800 and 950 cm^{-1} bands and a decrease in the vibration intensity of 580 cm^{-1} are observed.

https://doi.org/10.1021/acs.jpcc.2c00349
J. Phys. Chem. C 2022, 126, 7510−7516

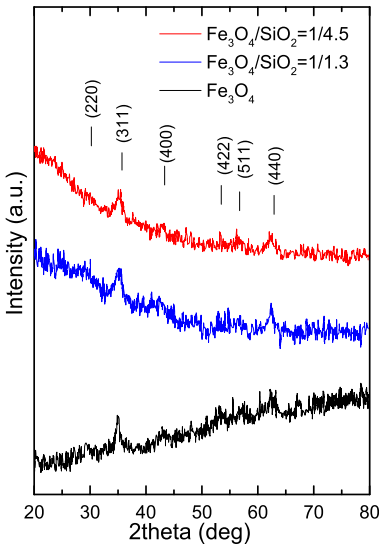

Figure 2. X-ray diffraction patterns of naked nanoparticles and nanoparticles coated with silica.

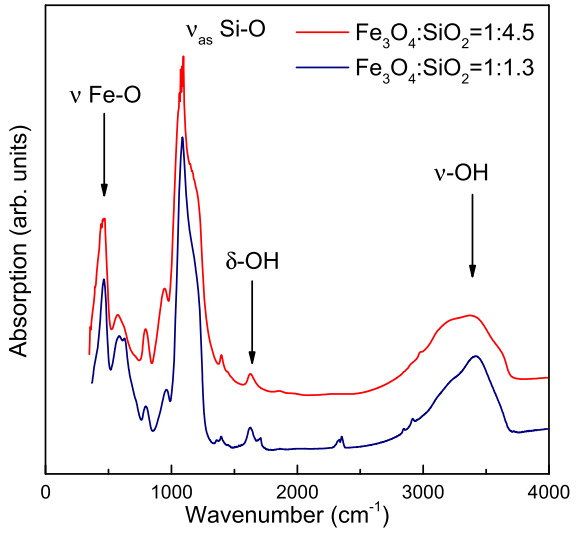

Figure 3. FTIR spectra of iron oxide nanoparticles coated with silica.

The data of magnetic measurements (Figure 4) provide information on the magnetic response of the particles, which is necessary for the analysis of the magnetic and magneto-mechanical response of the prepared composite particles. In addition, magnetic measurements are an additional source of information about the structure of particles.

The magnetization curves measured in the range from −15 to 15 kOe are symmetric about the origin and contain a reversible part as well as an irreversible part—a hysteresis loop (Figure 4). The coercive force, remanent magnetization, and magnetization in a field of 15 kOe decrease with increasing temperature. Low values of the coercive field indicate that particles with this size are close to the transition to the superparamagnetic state. The relatively small values of the saturation magnetization of nanoparticles are due to the silica shell. This can be used for an independent assessment of the ratio of magnetite and silica, originally made on the basis of the technological filling of the components during the synthesis. For such an estimation, we determined the magnetizations of the two studied samples of the composite material in a state of complete magnetic saturation and zero temperature (M_{s0}). As can be seen from Figure 5, the magnetization does not reach saturation even in the maximum fields used (15 kOe) and decreases with increasing temperature; therefore, we deter-

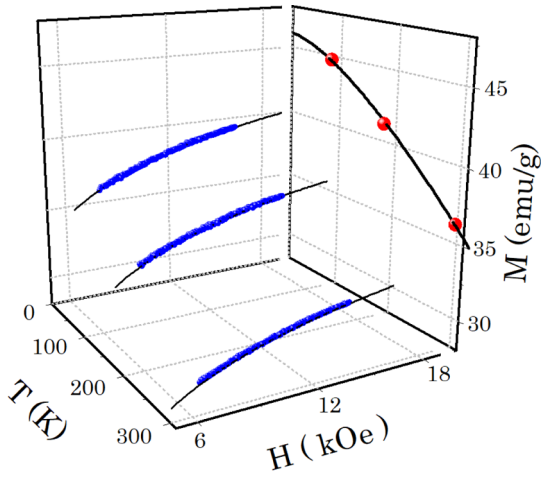

Figure 5. Determination of M_{s0} from the magnetization curves of particles in the region of magnetization approaching saturation. Blue symbols—measured M (H), thin black lines—fitting by eq 1, red symbols—saturation magnetization estimated from (1), and black thick line—description of $M_s(T)$ by eq 2.

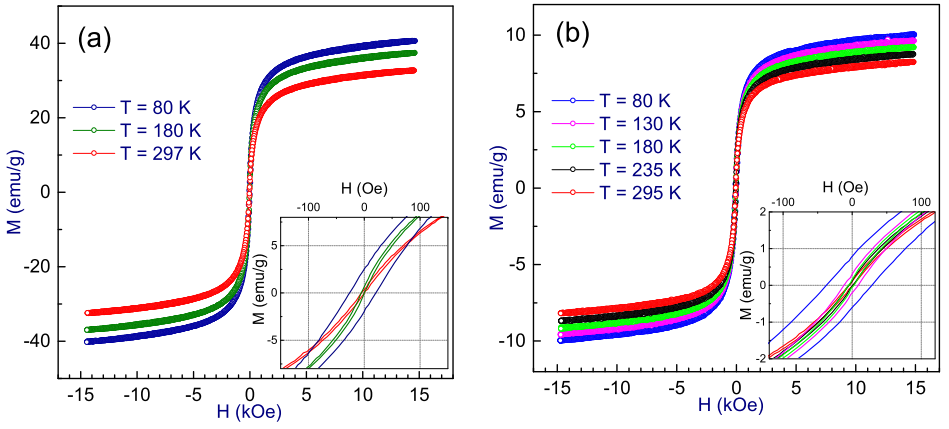

Figure 4. Hysteresis loops of magnetic nanoparticles. (a)—Fe_3O_4/SiO_2 = 1:1.3 and (b)—Fe_3O_4/SiO_2 = 1:4.5.

https://doi.org/10.1021/acs.jpcc.2c00349
J. Phys. Chem. C 2022, 126, 7510−7516

mined M_{s0} as follows. It was found that at a stabilized temperature in high fields, the magnetization of nanoparticles approaches saturation according to the equation[13−15]

$$M(H) = M_s\cdot\left(1 - \frac{1}{15}\frac{H_a^2}{H^{1/2}(H^{3/2} + H_R^{3/2})}\right) \quad (1)$$

where M_s is the saturation magnetization, H_a is the anisotropy field, and H_R is the exchange field in the core−shell system. Indeed, in our case, eq 1 makes it possible to describe the magnetization curves in high fields and estimate the quantitative values of Ms for different temperatures.

The change in the M_s value in magnetite nanoparticles with temperature is described by Bloch's law $T^{3/2}$[16]

$$M_s(T) = M_{s0}\cdot(1 - B\cdot T^{3/2}) \quad (2)$$

Extrapolation of the data to 0 K according to eq 2 (Figure 4) gives an estimate of M_{s0} (Table 1). Because the magnetization

Table 1. Saturation Magnetization of Particles at 0 K[a]

sample	X_m, at synthesis (from TEM)	M_{s0}, emu/g	estimate of M_{s0_m}, at synthesis (from TEM)
A	0.435 (0.588)	46.0 ± 0.2	105 (78.2)
B	0.182 (0.291)	10.9 ± 0.2	60 (37.5)

[a] X_m is the mass fraction of magnetite, M_{s0} is the saturation magnetization, and M_{s0_m} is the magnetite core magnetization.

of silica is zero, the magnetization of the composite particle is related to the weight fraction of magnetite nanoparticles X_m and their magnetization M_{s0_m} as $M_{s0} = X_m\cdot M_{s0\_m}$. Using the measured value M_{s0} and the weight fraction of magnetite X_m, we estimated that the magnetization of nanoparticles reduced only to the weight of magnetite M_{s0_m} (see Table 1). Table 1 shows the mass fraction of magnetite calculated from the synthesis and the corresponding magnetization of the magnetite core. In parentheses are the mass fraction and magnetization calculated from the TEM results. As is known, the magnetization of pure quasispherical magnetite nanoparticles M_{s0_m} is lower than the magnetization of bulk magnetite crystals (92 emu/g) and depends on their size. For particles with an average size of 10 nm (our case) and a thickness of the spin-glass shell of 1.7 nm,[17,18] according to ref,[19] the magnetization should be $M_{s0\_m} \approx 26$ emu/g. It can be seen from Table 1 that the magnetization of nanoparticles is significantly higher and that the magnetization of magnetite in the composition of the two studied samples is different. This can be interpreted as stoichiometric displacement in the composition of Fe_3O_4@SiO_2 nanoparticles from standard Fe_3O_4. In addition, we also find an indication that this stoichiometric displacement is different in samples with different weights of the magnetite and silica (the difference in magnetization in Table 1). Different stoichiometries in the magnetite mean that the stoichiometry of the silicate coating will also differ, that is, it will have varying potencies in the isolation of nucleic acids.

Based on the enthalpies of formation of bulk SiO_2 and Fe_3O_4,[20,21] oxygen should not move from the Fe_3O_4 core to the SiO_2 shell. Because the thickness of the silicate shell in sample A is several nanometers, one can expect its greater imperfection and, consequently, a different (including increased) reactivity. We assume that this activity is the reason for the deviation of the out-of-stoichiometry magnetite−maghemite series for sample A. The magnetization of sample B does not differ much from the literature data for nanoparticles of the magnetite−maghemite series[19,22] due to the fact that the properties of much thicker silica differ little from the properties of bulk SiO_2. This gives us a reason to assume that in the case of magnetite nanoparticles in a silica shell of nanometer thickness, we are dealing with a special result of chemical interaction associated with these nanometer scales of the core and shell.

The temperature behavior of the coercive force in Figure 6 does not follow the power-law dependence

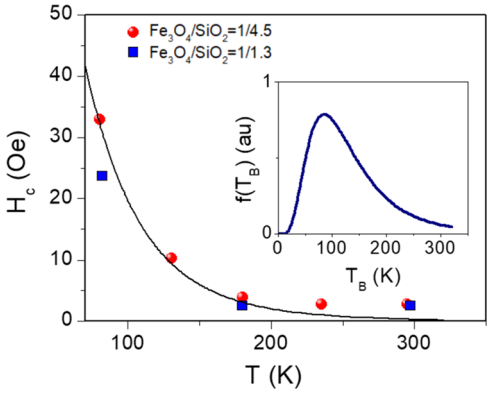

Figure 6. Temperature dependence of the coercive force. The inset shows the distribution of nanoparticles by blocking temperature.

$$H_c(T) = H_c(0)\cdot(1 - (T/T_B)^{\alpha}) \quad (3)$$

usually discussed for single-domain non-interacting nanoparticles at temperatures below the blocking temperature (T_B).[23,24] The power exponent α, in this case, is in the range from 0.67 to 1.00.[25,26] This deviation may be due to the inhomogeneity of the blocking temperature in the system of the studied nanoparticles. Therefore, to describe the coercive force, we used averaging[27]

$$H_c(T) = H_c(0)\cdot\frac{\int H_c(T)f(T_B)dT_B}{\int f(T_B)dT_B} \quad (4)$$

where the parameter $\langle H_c(0)\rangle$ is the average coercive force at T = 0 K. Describing the experimental behavior of the coercive force by expression (2), we can determine the parameters of the distribution function $f(T_B)$ corresponding to the best description of the experiment. The best agreement is achieved using the lognormal distribution function: $f(T_B) = \frac{1}{T_B\cdot\sigma\sqrt{2\pi}}\cdot\exp\left(-\ln^2\left(\frac{T_B}{T_{B0}}\right)/2\sigma^2\right)$ with the parameters T_{B0} = 85 K and σ = 0.55. This blocking temperature value is calculated from a number-weighted distribution. For practice, the volume-weighted distribution of particles is more important. The estimate of the volumetric average blocking temperature is $\langle T_B\rangle_V$ = 130 ± 20 K.

Figure 7 shows the $M(T)$ dependencies obtained in the ZFC/FC mode in the field H = 10 Oe. The dependencies obtained are typical for systems of superparamagnetic nanoparticles; a maximum of the ZFC dependence (T_{max}) is observed, as well as a bifurcation of the FC and ZFC dependencies (T_{irr}). For the A sample, the T_{max} and T_{irr} values were 129 and 147 K, respectively. For the B sample, the T_{max} and T_{irr} values were 144 and 172 K, respectively. The obtained

https://doi.org/10.1021/acs.jpcc.2c00349
J. Phys. Chem. C 2022, 126, 7510−7516

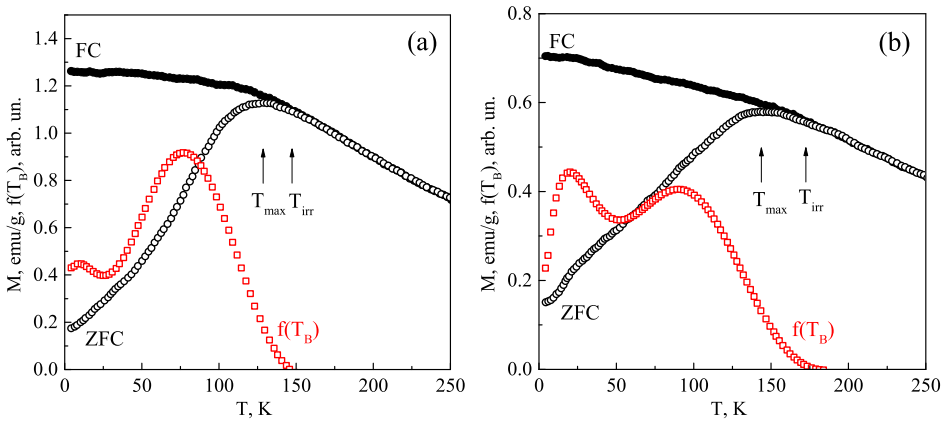

Figure 7. $M(T)$ dependencies measured in the ZFC/FC mode and dependencies $f(T_B) \sim d(M(T)_{ZFC} - M(T)_{FC})/dT$. (a)—$Fe_3O_4/SiO_2$ = 1:1.3 and (b)—Fe_3O_4/SiO_2 = 1:4.5.

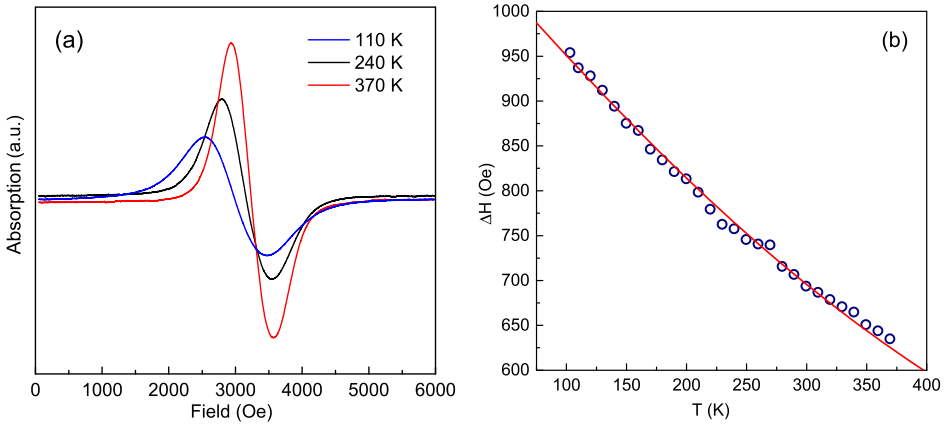

Figure 8. (a) FMR spectra and (b) temperature dependence of the FMR line width.

temperatures differ from the same temperatures for uncoated nanoparticles.[22] This difference is due to the presence of a silicate shell.

The size and blocking temperature distribution of nanoparticles can be estimated using the dependence $d(M(T)_{ZFC} - M(T)_{FC})/dT$. The maximum of this dependence can be considered as the average blocking temperature. For nanoparticles with a thin shell, the $f(T_B)$ dependence has a maximum at 77 K, while for particles with a thick shell, two maxima are observed at 20 and 90 K. As a result, we see that the estimate of the blocking temperature from the $M(T)$ dependencies is in good agreement with the previous estimate from $H_C(T)$.

FMR spectra measured in the temperature range 110−370 °C are shown in Figure 8. With increasing temperature, a decrease in the FMR line width, an increase in the resonance field, and the intensity of resonant absorption are observed.

According to ref 28 29, in an ensemble of chaotically oriented ferrimagnetic nanoparticles, the absorption line width is a function of temperature $\Delta H(T) = \Delta H_S(T) + \Delta H_U(T)$, where $\Delta H_S(T)$ is the contribution to broadening due to superparamagnetism of nanoparticles and $\Delta H_U(T)$ is the contribution to the broadening due to the scatter of the directions of the anisotropy fields of the particles.

These two contributions are described as follows

$$\Delta H_S(T) = \frac{2}{\sqrt{3}} \frac{\omega}{\gamma} \frac{\alpha(x - L_1)}{xL_1}$$

$$\text{and } \Delta H_U(T) = 3\frac{K}{M}\frac{L_2}{L_1}$$

where $x = \omega/\gamma MV/kT$ is the Langevin parameter, M is the magnetization, V is the particle volume, k is the Boltzmann constant, T is the temperature, ω is the frequency, γ is the gyromagnetic ratio, $L_{1,2}$ is the Langevin functions, and K is the anisotropy constant.

Figure 8b shows the values of the FMR line width of nanoparticles depending on temperature and the result of fitting the experimental data. The FMR line width was determined as the distance between two peaks on the differential resonance absorption curve. The theoretical curve shown in Figure 8b is characterized by two fitting parameters: $K_{eff}V = 6.95 \times 10^{-14}$ erg and $MV = 5.7 \times 10^{-17}$ emu. Assuming that the magnetization of nanoparticles is 370 G, the nanoparticle size and anisotropy constant can be calculated. Thus, the size is 6.7 nm and the anisotropy constant is $K_{eff} = 4.4 \times 10^5$ erg/cm^3. The deviation of the average size of nanoparticles from the results of electron microscopy can be explained by the fact that atoms of the surface-disordered layer do not participate in FMR.

To assess the ability of the obtained nanoparticles to bind DNA, they were used as a replacement for a silicate sorbent in the commercial reagent kit for DNA isolation DNA-sorb B

https://doi.org/10.1021/acs.jpcc.2c00349
J. Phys. Chem. C 2022, 126, 7510−7516

(AmpliSens, Russia). Some modifications in the manufacturer's protocol of the isolation procedure were published earlier and included the absence of particle heating both at the stage of drying and at the stage of DNA elution. Elution was carried out with preheated TE buffer.[30] The result of approbation showed that 1:1.3 nanoparticles allow the isolation of an equal or a smaller number of molecules in comparison with standard silica per 1 mg of sorbent. However, the further use of the isolated DNA for genetic testing by the polymerase chain reaction method demonstrated the inhibitory effect of nanoparticles on the reaction enzyme (DNA polymerase). DNA isolation with 1:4.5 particles made it possible to isolate up to 3.6 times more DNA per 1 mg of sorbent, and the inhibitory effect was not observed in further studies.[30]

4. CONCLUSIONS

In this work, silica-coated magnetite nanoparticles with different shell thicknesses have been investigated. Magnetometric studies have shown that the magnetization of magnetite cores of synthesized Fe_3O_4@SiO_2 nanoparticles is significantly higher than that of bulk magnetite and that the magnetization of magnetite in the composition of the two studied samples is different. This can be interpreted as stoichiometric displacement in the composition of Fe_3O_4@SiO_2 nanoparticles from standard Fe_3O_4. The stoichiometric displacement depends on the silica to magnetite ratio. A larger deviation in a sample with a thinner shell is due to a chemical interaction of the nanosized shell and core. The nanoparticle blocking temperatures were determined both from the ZFC/FC dependencies and from the temperature dependence of the coercive force. The obtained blocking temperatures are in good agreement. Analysis of the temperature dependence of the FMR line width made it possible to determine the values of the constant of effective anisotropy and magnetization of an individual particle: $K_{eff}V = 6.95 \times 10^{-14}$ erg and $MV = 5.7 \times 10^{-17}$ emu. Thicker-coated nanoparticles show greater efficiency in DNA isolation and do not damage molecules due to complete magnetite coverage.

AUTHOR INFORMATION

Corresponding Author

Roman N. Yaroslavtsev − *Krasnoyarsk Scientific Center, Federal Research Center KSC SB RAS, Krasnoyarsk 660036, Russia;* orcid.org/0000-0002-6791-7492; Email: yarman@bk.ru

Authors

Sergey V. Stolyar − *Krasnoyarsk Scientific Center, Federal Research Center KSC SB RAS, Krasnoyarsk 660036, Russia; Siberian Federal University, Krasnoyarsk 660041, Russia; Kirensky Institute of Physics, Federal Research Center KSC SB RAS, Krasnoyarsk 660036, Russia*

Anna V. Tyumentseva − *Krasnoyarsk Scientific Center, Federal Research Center KSC SB RAS, Krasnoyarsk 660036, Russia*

Sergey V. Komogortsev − *Kirensky Institute of Physics, Federal Research Center KSC SB RAS, Krasnoyarsk 660036, Russia; Reshetnev Siberian State University of Science and Technology, Krasnoyarsk 660049, Russia*

Ekaterina S. Tyutrina − *Krasnoyarsk Scientific Center, Federal Research Center KSC SB RAS, Krasnoyarsk 660036, Russia*

Alina T. Saitova − *Krasnoyarsk Scientific Center, Federal Research Center KSC SB RAS, Krasnoyarsk 660036, Russia;* orcid.org/0000-0002-5921-0745

Yulia V. Gerasimova − *Kirensky Institute of Physics, Federal Research Center KSC SB RAS, Krasnoyarsk 660036, Russia*

Dmitriy A. Velikanov − *Kirensky Institute of Physics, Federal Research Center KSC SB RAS, Krasnoyarsk 660036, Russia*

Michael V. Rautskii − *Kirensky Institute of Physics, Federal Research Center KSC SB RAS, Krasnoyarsk 660036, Russia*

Rauf S. Iskhakov − *Kirensky Institute of Physics, Federal Research Center KSC SB RAS, Krasnoyarsk 660036, Russia*

Complete contact information is available at: https://pubs.acs.org/10.1021/acs.jpcc.2c00349

Notes

The authors declare no competing financial interest.

ACKNOWLEDGMENTS

This work was supported by the Russian Science Foundation and the Krasnoyarsk Region Science and Technology Support Fund, grant No. 22-14-20020. We are grateful to the Center of collective use of FRC KSC SB RAS for the provided equipment.

REFERENCES

(1) Stolyar, S. V.; Balaev, D. A.; Krasikov, A. A.; Dubrovskiy, A. A.; Yaroslavtsev, R. N.; Bayukov, O. A.; Volochaev, M. N.; Iskhakov, R. S. Modification of the Structure and Magnetic Properties of Cobalt-Doped Ferrihydrite Nanoparticles Under Heat Treatment. *J. Supercond. Nov. Magnetism* **2018**, *31*, 1133−1138.

(2) Berry, C. C.; Curtis, A. S. G. Functionalisation of Magnetic Nanoparticles for Applications in Biomedicine. *J. Phys. D Appl. Phys.* **2003**, *36*, R198−R206.

(3) Chilom, C. G.; Sandu, N.; Bălăşoiu, M.; Yaroslavtsev, R. N.; Stolyar, S. V.; Rogachev, A. V. Ferrihydrite Nanoparticles Insights: Structural Characterization, Lactate Dehydrogenase Binding and Virtual Screening Assay. *Int. J. Biol. Macromol.* **2020**, *164*, 3559−3567.

(4) Tartaj, P.; Morales, M. a. d. P.; Veintemillas-Verdaguer, S.; lez-Carre o, T. G.; Serna, C. J. The Preparation of Magnetic Nanoparticles for Applications in Biomedicine. *J. Phys. D Appl. Phys.* **2003**, *36*, R182−R197.

(5) Tolmacheva, V. V.; Apyari, V. V.; Kochuk, E. V.; Dmitrienko, S. G. Magnetic Adsorbents Based on Iron Oxide Nanoparticles for the Extraction and Preconcentration of Organic Compounds. *J. Anal. Chem.* **2016**, *71*, 321−338.

(6) Borlido, L.; Azevedo, A. M.; Roque, A. C. A.; Aires-Barros, M. R. Magnetic Separations in Biotechnology. *Biotechnol. Adv.* **2013**, *31*, 1374−1385.

(7) Yarjanli, Z.; Ghaedi, K.; Esmaeili, A.; Rahgozar, S.; Zarrabi, A. Iron Oxide Nanoparticles May Damage to the Neural Tissue through Iron Accumulation, Oxidative Stress, and Protein Aggregation. *BMC Neurosci.* **2017**, *18*, 51.

(8) Gaharwar, U. S.; Meena, R.; Rajamani, P. Iron Oxide Nanoparticles Induced Cytotoxicity, Oxidative Stress and DNA Damage in Lymphocytes. *J. Appl. Toxicol.* **2017**, *37*, 1232−1244.

(9) Bag, S.; Rauwolf, S.; Schwaminger, S. P.; Wenzel, W.; Berensmeier, S. DNA Binding to the Silica: Cooperative Adsorption in Action. *Langmuir* **2021**, *37*, 5902−5908.

(10) Shao, D.; Xia, A.; Hu, J.; Wang, C.; Yu, W. Monodispersed Magnetite/Silica Composite Microspheres: Preparation and Application for Plasmid DNA Purification. *Colloids Surf. A Physicochem. Eng. Asp.* **2008**, *322*, 61−65.

(11) Chiang, C.-L.; Sung, C.-S.; Wu, T.-F.; Chen, C.-Y.; Hsu, C.-Y. Application of Superparamagnetic Nanoparticles in Purification of Plasmid DNA from Bacterial Cells. *J. Chromatogr. B* **2005**, *822*, 54−60.

(12) Komina, A. V.; Yaroslavtsev, R. N.; Gerasimova, Y. V.; Stolyar, S. V.; Olkhovsky, I. A.; Bairmani, M. S. Magnetic Nanoparticles for Extracting DNA from Blood Cells. *Bull. Russ. Acad. Sci. Phys.* **2020**, *84*, 1362−1365.
(13) Komogortsev, S. V.; Stolyar, S. V.; Chekanova, L. A.; Yaroslavtsev, R. N.; Bayukov, O. A.; Velikanov, D. A.; Volochaev, M. N.; Eroshenko, P. E.; Iskhakov, R. S. Square Plate Shaped Magnetite Nanocrystals. *J. Magn. Magn. Mater.* **2021**, *527*, 167730.
(14) Stolyar, S. V.; Komogortsev, S. V.; Chekanova, L. A.; Yaroslavtsev, R. N.; Bayukov, O. A.; Velikanov, D. A.; Volochaev, M. N.; Cheremiskina, E. V.; Bairmani, M. S.; Eroshenko, P. E.; et al. Magnetite Nanocrystals with a High Magnetic Anisotropy Constant Due to the Particle Shape. *Tech. Phys. Lett.* **2019**, *45*, 878−881.
(15) Blyakhman, F. A.; Makarova, E. B.; Shabadrov, P. A.; Fadeyev, F. A.; Shklyar, T. F.; Safronov, A. P.; Komogortsev, S. V.; Kurlyandskaya, G. V. Magnetic Nanoparticles as a Strong Contributor to the Biocompatibility of Ferrogels. *Phys. Met. Metallogr.* **2020**, *121*, 299−304.
(16) Komogortsev, S. V.; Stolyar, S. V.; Chekanova, L. A.; Yaroslavtsev, R. N.; Bayukov, O. A.; Velikanov, D. A.; Volochaev, M. N.; Eroshenko, P. E.; Iskhakov, R. S. Square Plate Shaped Magnetite Nanocrystals. *J. Magn. Magn. Mater.* **2021**, *527*, 167730.
(17) Kim, T.; Shima, M. Reduced Magnetization in Magnetic Oxide Nanoparticles. *J. Appl. Phys.* **2007**, *101*, 09M516.
(18) Beketov, I. V.; Safronov, A. P.; Medvedev, A. I.; Alonso, J.; Kurlyandskaya, G. V.; Bhagat, S. M. Iron Oxide Nanoparticles Fabricated by Electric Explosion of Wire: Focus on Magnetic Nanofluids. *AIP Adv.* **2012**, *2*, 022154.
(19) Safronov, A. P.; Beketov, I. V.; Komogortsev, S. V.; Kurlyandskaya, G. V.; Medvedev, A. I.; Leiman, D. V.; Larrañaga, A.; Bhagat, S. M. Spherical Magnetic Nanoparticles Fabricated by Laser Target Evaporation. *AIP Adv.* **2013**, *3*, 052135.
(20) Chase, M. W., Jr. *NIST-JANAF Themochemical Tables*, 4th ed.; American Chemical Society, 1998.
(21) Zumdahl, S. S. *Chemical Principles*, 6th ed; Cengage Learning, 2005.
(22) Dutta, P.; Pal, S.; Seehra, M. S.; Shah, N.; Huffman, G. P. Size Dependence of Magnetic Parameters and Surface Disorder in Magnetite Nanoparticles. *J. Appl. Phys.* **2009**, *105*, 07B501.
(23) Iskhakov, R. S.; Komogortsev, S. V.; Stolyar, S. V.; Prokof'ev, D. E.; Zhigalov, V. S. Structure and Magnetic Properties of Nanocrystalline Condensates of Iron Obtained by Pulse Plasma Evaporation. *Phys. Met. Metallogr.* **1999**, *88*, 261−269.
(24) Komogortsev, S. V.; Iskhakov, R. S.; Balaev, A. D.; Kudashov, A. G.; Okotrub, A. V.; Smirnov, S. I. Magnetic Properties of Fe3C Ferromagnetic Nanoparticles Encapsulated in Carbon Nanotubes. *Phys. Solid State* **2007**, *49*, 734−738.
(25) Pfeiffer, H. Determination of Anisotropy Field Distribution in Particle Assemblies Taking into Account Thermal Fluctuations. *Phys. Status Solidi* **1990**, *118*, 295−306.
(26) Poperechny, I. S.; Raikher, Y. L.; Stepanov, V. I. Dynamic Hysteresis of a Uniaxial Superparamagnet: Semi-Adiabatic Approximation. *Phys. B Condens. Matter* **2014**, *435*, 58−61.
(27) Komogortsev, S. V.; Iskhakov, R. S.; Balaev, A. D.; Okotrub, A. V.; Kudashov, A. G.; Momot, N. A.; Smirnov, S. I. Influence of the Inhomogeneity of Local Magnetic Parameters on the Curves of Magnetization in an Ensemble of Fe3C Ferromagnetic Nanoparticles Encapsulated in Carbon Nanotubes. *Phys. Solid State* **2009**, *51*, 2286−2291.
(28) Raikher, Y. L.; Stepanov, V. I. Thermal Fluctuation Effect on the Ferromagnetic-Resonance Line-Shape in Disperse Ferromagnets. *JETP Lett.* **1992**, *102*, 1409−1423.
(29) Poperechny, I. S.; Raikher, Y. L. Ferromagnetic Resonance in Uniaxial Superparamagnetic Particles. *Phys. Rev. B: Condens. Matter Mater. Phys.* **2016**, *93*, 014441.
(30) Tyumentseva, A. V.; Yaroslavtsev, R. N.; Stolyar, S. V.; Saitova, A. T.; Tyutrina, E. S.; Gorbenko, A. S.; Stolyar, M. A.; Olkhovskiy, I. A. Silica-Coated Iron Oxide Nanoparticles for DNA Isolation for Molecular Genetic Studies in Hematology. *Genet. Test. Mol. Biomarkers* **2021**, *25*, 611−614.

https://doi.org/10.1021/acs.jpcc.2c00349
J. Phys. Chem. C 2022, 126, 7510−7516